Biomedicine & Pharmacotherapy 128 (2020) 110243

Contents lists available at ScienceDirect

Biomedicine & Pharmacotherapy

journal homepage: www.elsevier.com/locate/biopha

Original article

Piperlongumine induces ROS mediated cell death and synergizes paclitaxel in human intestinal cancer cells

Laxminarayan Rawat[a], Harsha Hegde[b], Sugeerappa Laxmanappa Hoti[b], Vijayashree Nayak[a,*]

[a] Department of Biological Sciences, Birla Institute of Technology and Science, Pilani, K.K. Birla Goa Campus, NH-17B, Zuarinagar, Goa 403726, India
[b] ICMR-National Institute of Traditional Medicine, Nehru Nagar, Belagavi, 590010, Karnataka, India

ARTICLE INFO

Keywords:
Piperlongumine
Smad4
Herbal medicine
Paclitaxel
Cancer
ROS

ABSTRACT

Piperlongumine (PL), a herbal drug extracted from long pepper (*Piper longum* L), is known for its anti-inflammatory and anti-cancer properties. Although, its anti-cancer potential has been evaluated in cancer models like breast, pancreatic, gastric, hepatocellular and lung carcinoma, there is no report on its bio-activity evaluation in intestinal cancers. Here, we report the anti-neoplastic potential of PL against human intestinal carcinoma *in-vitro* and its possible mechanisms of action. Cytotoxicity studies demonstrate that PL inhibits cell proliferation of INT-407 and HCT-116 cells in a concentration and time-dependent manner. Also, PL elevated the levels of intracellular reactive oxygen species, which may lead to lethal oxidative stress, mitochondrial dysfunction, and nuclear fragmentation. Remarkably, *P53, P21, BAX*, and *SMAD4* were significantly upregulated after PL treatment whereas; *BCL2* and *SURVIVIN* were down-regulated. Moreover, the combination study also shows the synergistic effect of PL with the current chemotherapeutic drug paclitaxel. These findings suggest that PL possesses anti-neoplastic properties in intestinal cancer cells.

1. Introduction

Intestinal carcinoma is one of the leading cause of cancer related mortality worldwide [1]. Various factors are responsible for carcinogenesis including age, family history, lifestyle, food, smoking and alcohol consumption [2,3]. Genetic alterations and unregulated proliferation are the primary characteristic of the cancer cells that leads to tumorigenesis [4]. Carcinogenesis and apoptosis are two opposite phenomena, but reactive oxygen species (ROS) have been reported to play a critical role in both. ROS may be produced by UV radiation, toxic chemicals and drugs, whereas the intracellular ROS is generated as byproducts of normal metabolism. The variation in intracellular ROS level triggers different cellular processes. At lower concentrations, ROS acts as a signaling molecule for several signal transductions [5,6] while at higher levels it causes lethality [7]. In order to overcome the intracellular oxidative stress, the cells activate their antioxidant machinery comprised of antioxidant enzymes and antioxidant metabolites. Cancer cells usually have elevated ROS and high levels of antioxidant system [8]. Since, the excessive oxidative stress induces apoptosis and eventually cell death. The increased ROS production in the presence of anti-cancer drugs like paclitaxel, 2-methoxyestradiol and trisenox, has been implicated to their anticancer potentials [9–11]. For further improvement in the specificity and efficacy of existing drugs and to control the side effects from the present generation of chemotherapy and radiotherapy, several herbal compounds have been inducted in management of cancer therapy. Recently Piperlongumine (PL) is identified as a biologically active alkaloid majorly found in long pepper (*Piper longum* L). It is a potent cytotoxic compound for malignant cells and traditionally used for the treatment of several diseases like malaria, viral hepatitis, gastrointestinal and common respiratory problems [12]. PL selectively induces ROS production in cancerous cells, which makes it a novel therapeutic agent to kill cancer cells without harming normal one [13]. PL activates p38, Akt, JNK, Erk, which promote protein glutathionylation or NFκB inhibition in different types of carcinomas [14–19]. However, the precise mechanism of action is not been fully understood in intestinal cancer. TGF-β signaling plays multiple roles in cancer progression depending on tumor stages and types [20]. It acts as either tumor suppressor or promoter depending on the SMAD and non-SMAD pathways respectively [21,22]. The patients with elevated SMAD4 expression have significantly better therapeutic response and survival as compared to patients with low level of SMAD4 in colorectal cancer [23,24]. Therefore, the therapeutic potential of PL in intestinal cancer would be worth understanding. Here, we report the anticancer potential of PL in intestinal cancer cell lines. We demonstrated that PL induces oxidative stress and thereby bring about the molecular and cellular changes that are potentially detrimental to the survival of cancer cells.

* Corresponding author.
E-mail addresses: lnrawat9@gmail.com (L. Rawat), drhvhegde@gmail.com (H. Hegde), slhoti@yahoo.com (S.L. Hoti), vijayashreenayak@gmail.com (V. Nayak).

https://doi.org/10.1016/j.biopha.2020.110243
Received 26 September 2019; Received in revised form 2 May 2020; Accepted 10 May 2020

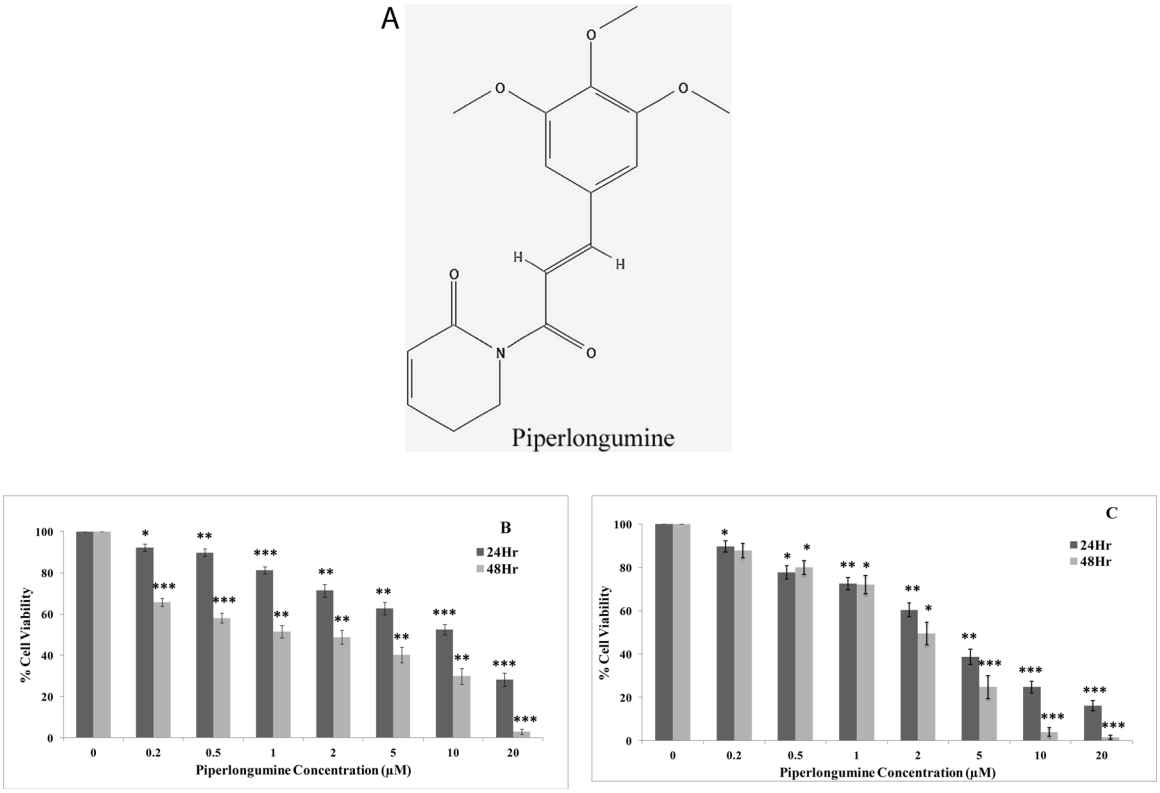

Fig. 1. (A) Chemical structure of piperlongumine. Cells were treated with increasing concentrations of PL (0–20 μM) for 24 and 48 h respectively. MTT test was performed to determine the proliferation of the cells. The histograms indicate percentage cell viability of INT-407 (B) and HCT-116 (C) cells after PL treatment. Data represented as the mean ± SE of 4 independent experiments (statistically significant differences, $*P < 0.05$, $** P < 0.01$, $*** P < 0.001$).

2. Materials and methods

Reagents: Dulbecco's Modified Eagle medium (DMEM) high glucose, Fetal bovine serum (FBS), 10X Phosphate buffer saline (PBS), 100X Antibiotic Antimycotic solution (penicillin (10 − 12 mg/mL)/ streptomycin (10000–12000 U/mL)/amphotericin (25–30 μg/ml)), Gentamicin (10 mg/mL) and trypsin-EDTA solution (0.25% Trypsin and 0.02% EDTA) were purchased from HIMEDIA laboratories (Mumbai, India). Piperlongumine (PL), Trypan Blue solution, Methylthiazolyldiphenyl-tetrazolium bromide (MTT), 2′,7′-Dichlorofluorescin diacetate (DCFDA), Acridine orange, Propidium iodide and Hoechst 33258 were purchased from Sigma-Aldrich Pvt. Ltd. (US). High-Capacity cDNA Reverse Transcription Kit, PCR Master Mix and SYBR™ Green Mix were purchased from Thermo Fisher Scientific (US). RNASure Mini Kit was purchased from Gentrix biotech (India). INT-407 and HCT-116 intestinal cancer cell lines were obtained from cell repository, National Centre for Cell Science, Pune, India. All reagents used were of analytical and molecular grade.

2.1. Cell culture

Two types of intestinal cancerous cells lines i.e. INT-407 and HCT-116 were used for this study. All the cell lines were grown in DMEM culture media supplemented with 10% FBS and 1X penicillin/streptomycin/amphotericin and were maintained at 37 °C in humidified incubator containing 5% CO_2.

2.2. Cell proliferation assay

Cultured cells were trypsinized and seeded in a 96- well plate at a density of 1×10^4 cells/well and incubated overnight. The cells were treated with PL (0, 0.2, 0.5, 1, 2, 5, 10 and 20 μM) and incubated for 24 and 48 h. After treatment, the media was removed and 50 μL of MTT solution (5 mg/mL) was added and the cells were incubated for another 3 h in CO_2 incubator. MTT was discarded and 100 μL of Dimethyl sulfoxide was added to dissolve the formazan crystals. Then, the absorbance was recorded at 570 nm using the Multiskan™ GO Microplate spectrophotometer (Thermo scientific, US). The ED50plus v1.0 tool was used to calculate mean inhibitory concentration (IC_{50}). For drug combination studies, the cells were co-treated with PL (1, 2.5 and 5 μM) and PTX (0.1, 0.5 and 1 μM) for 24 h. MTT assay was performed to determine the cell viability. The data was analyzed using SynergyFinder and CompuSyn software [25–27]. For all the experiments, the untreated cells were considered as control.

2.3. Cell viability assay

Cell viability assays were performed using acridine orange and propidium iodide double-staining method. In brief, INT-407 and HCT-116 cells were seeded at a density of 1×10^5 cells/well in a 12-well plate and incubated overnight. The cells were exposed to defined concentrations of PL (0, 1 μM, 13 μM for INT-407, 8 μM for HCT-116, and 20 μM) for 24 h. Media was removed and the cells were washed with 1X PBS. A volume of 300 μL of 100μM Acridine orange and Propidium iodide (1:1) was added to the cells and incubated at room temperature (RT) for 15 min under dark condition. The Stain was discarded and the cells were re-washed with 1X PBS twice. The stained cells were observed under the fluorescence microscope (CKX53, Olympus, Japan) and number of viable/dead cells were counted [28].

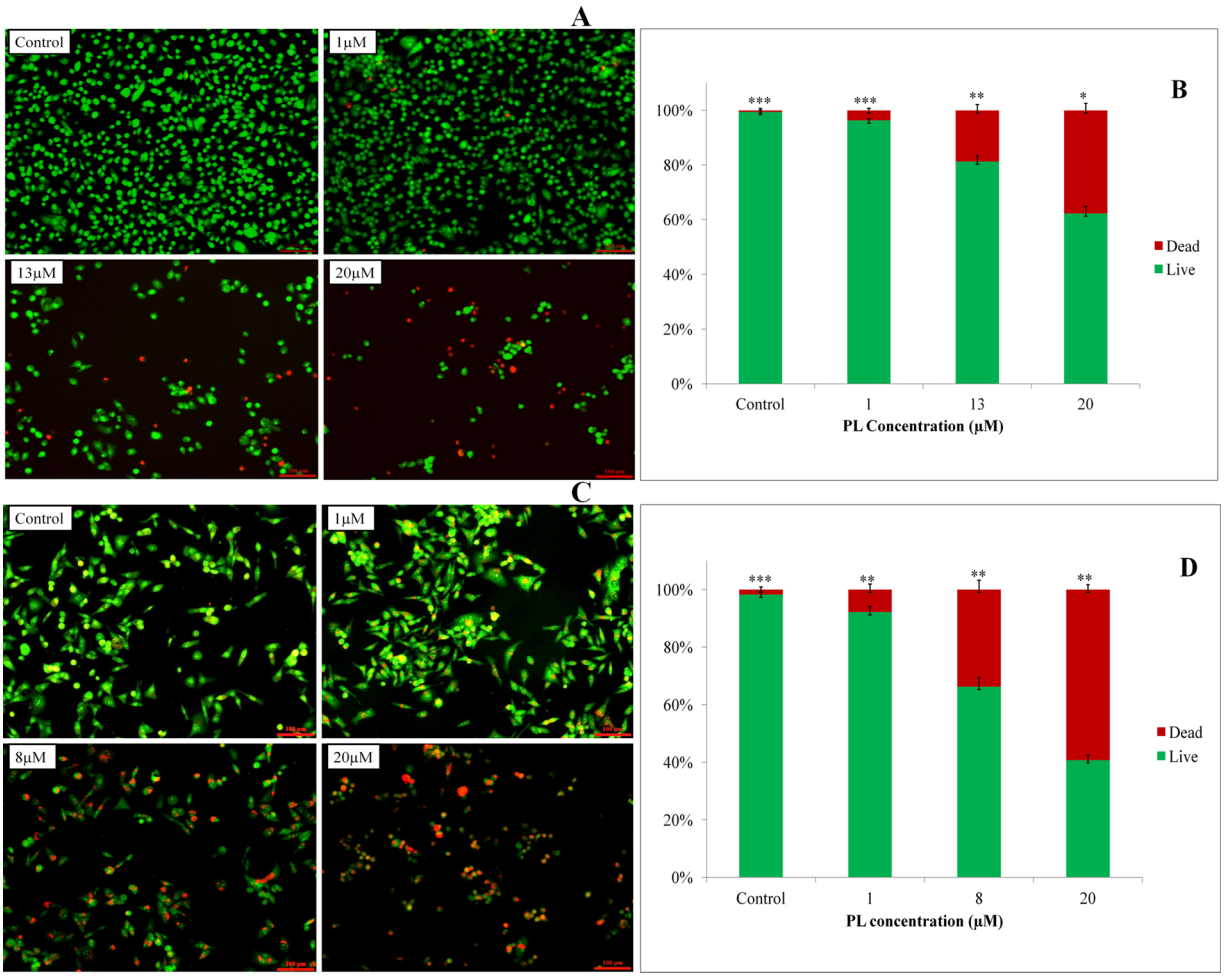

Fig. 2. Acridine orange and Propidium iodide double staining was performed after 24 h PL treatment. Representative fluorescence images of INT-407 (A) and HCT-116 (C) cells. (B) & (D) show the quantified data of (A) & (C) respectively. The Green fluorescence represents viable whereas red fluorescence represents the dead cells. Data represented as the mean ± SE of three independent experiments (statistically significant differences, * $P < 0.05$, ** $P < 0.01$, *** $P < 0.001$).

2.4. Assessment of nuclear morphology by Hoechst 33258

INT-407 and HCT-116 cells were seeded on the coverslips placed in a 12-well plate with density of 1×10^5 cells/well and allowed to adhere overnight. The cells were treated with PL (0, 1 μM, 13 μM for INT-407 and 8 μM for HCT-116) for 24 h. Media was discarded and cells were washed with 1X PBS. Fixation was done using freshly-prepared 4% formaldehyde solution at RT for 15 min. Following the fixation, formaldehyde was discarded and the cells were washed with 1X PBS. Then, 800 μL of tritonX-100 (0.01%) was added and the cells were incubated for 10 min at RT. Triton X-100 was removed and cells were washed with 1X PBS. Finally, the cells were stained with Hoechst 33258 (1 μg/mL) and incubated for 15 min at RT under dark condition. The stain was removed and the cells were washed twice with 1X PBS to reduce over staining. Coverslips were mounted on slides with the help of vectashield antifade mounting medium. The morphology of the nuclei was visualized under confocal laser scanning microscope (FV3000, Olympus Corporation, Japan) [29].

2.5. Quantitation of ROS by 2′,7′-Dichlorofluorescin diacetate (DCFDA) assay

The intracellular ROS levels were quantified with oxidation-sensitive DCFDA reagent. Cells were seeded in a 12-well plate at 1×10^5 seeding and were allowed to grow overnight. Cells were treated with PL (0, 1 μM, 13 μM for INT-407, 8 μM for HCT-116, and 20 μM) for 24 h. After PL treatment, 30 μL of 10 μM DCFDA was added and the cells were kept at 37 °C for 30 − 40 min under dark conditions. Cells were then visualized under fluorescence microscope (CKX53, Olympus, Japan) [30].

2.6. Wound healing assay

Migration of cancer cells was assessed by wound healing assay. For this, 1×10^5 cells/well were seeded in a 12-well plate and were allowed to grow for 24 h in DMEM supplemented with 4% FBS. A single line scratch was made in monolayer culture with a sterile micropipette tip (200 μL) and the floating cells were washed out with 1X PBS. Defined concentration of PL (0, 1 μM, 13 μM for INT-407, 8 μM for HCT-116, and 20 μM) were added to the cells and each scratch was visualized and the images were captured at different time points 0, 12 and 24 h [31].

2.7. RNA expression analysis by real time PCR

For the isolation of total RNA, the cells were treated with PL (0,

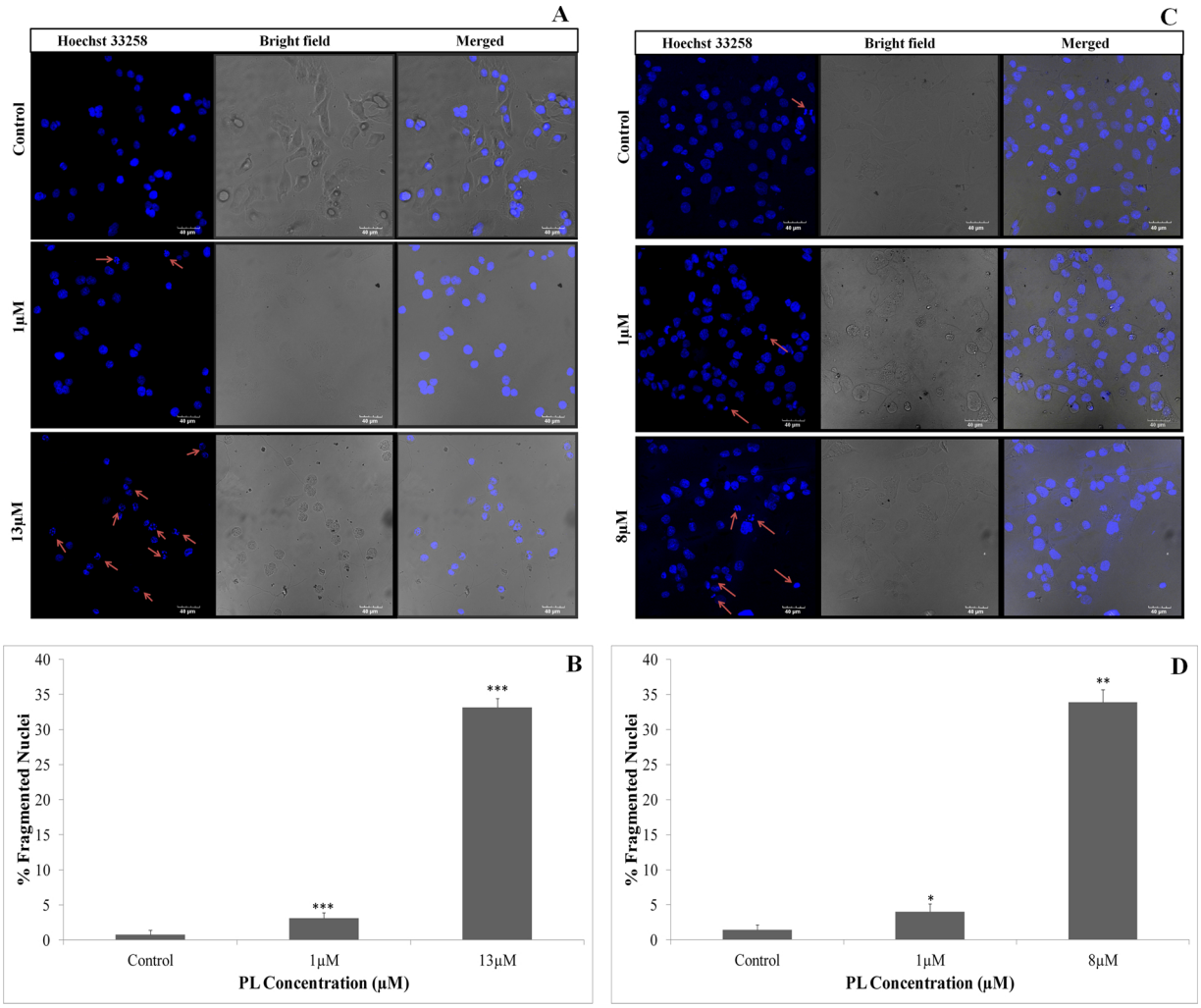

Fig. 3. Morphological changes of cell nuclei were analyzed by Hoechst 33258 staining after 24 h PL treatment. Representative fluorescence images of INT-407 (A) and HCT-116 (C) cells nuclei. (B) & (D) represent the quantified data of (A) & (C) respectively. Arrow indicates the chromatin condensation and nuclear fragmentation. Data represented as the mean ± SE of three independent experiments (statistically significant differences, * $P < 0.05$, ** $P < 0.01$, *** $P < 0.001$).

13 μM for INT-407 and 8 μM for HCT-116) for 24 h were used. The total RNA was extracted using the RNASure Mini Kit (Genetrix, India). The concentration and purity of extracted RNA was quantified using the Nanodrop spectrophotometer (Thermo Fisher Scientific, US). The cDNA was synthesized using high capacity cDNA synthesis kit (Applied Biosystems, US). Q-PCR was performed in a total volume of 20 μL, with 10 μL of 2 × SYBR Green QPCR Master Mix (Agilent Technologies), 1 μL each of forward and reverse primers (10 pM), 2 μL cDNA (25 ng/μL) and 6 μL ddH_2O. Q-PCR was performed using AriaMx Real-time PCR System (Agilent Technologies Inc., USA) with cycling conditions as follows: Initial denaturation at 95 °C for 3 min; followed by 40 cycles of denaturation at 95 °C for 30 s, 55 °C for 40 s and 72 °C for 60 s. The melting curves were analyzed to confirm specificity of primers. Relative mRNA expression or fold change was quantified using the $2^{-\Delta\Delta CT}$ method and normalized with human 18 s rRNA [32]. All the primers used in this study are included in Supplementary file 1.

2.8. Statistical data analysis

For each sample, three biological replicates and three technical replicates were analyzed. All data are presented as means with standard deviation and were analyzed using the Two-way ANOVA or Student's *t*-test. The *P* values are represented in the figures as follows: *$P < 0.05$; **$P < 0.01$; ***$P < 0.001$; ns, not significant.

3. Results

3.1. Piperlongumine shows cytotoxicity in intestinal cancer cells

The cytotoxicity of piperlongumine (PL) was tested in INT-407 and HCT-116 human intestinal cancer cells *in vitro*. The results showed the PL dose and treatment time dependent growth inhibition in both the cell lines (Fig. 1B and C). For instance, 10 μM of PL could inhibit the growth of INT-407 cells by 48% and 70.2% in 24 h and 48 h of treatment respectively. While the HCT-116 cells showed better response to PL and growth inhibition was 75.3% and 96% in 24 h and 48 h treatment respectively. Furthermore, the cells treated with 20 μM PL, the growth inhibition for both the cell lines was more than 95% in 48 h. The half maximal inhibitory concentration (IC_{50}) of PL for INT-407 was observed to be 13 μM and 9 μM while for HCT-116 cells it was 8 μM and 6 μM after 24 h and 48 h incubation, respectively.

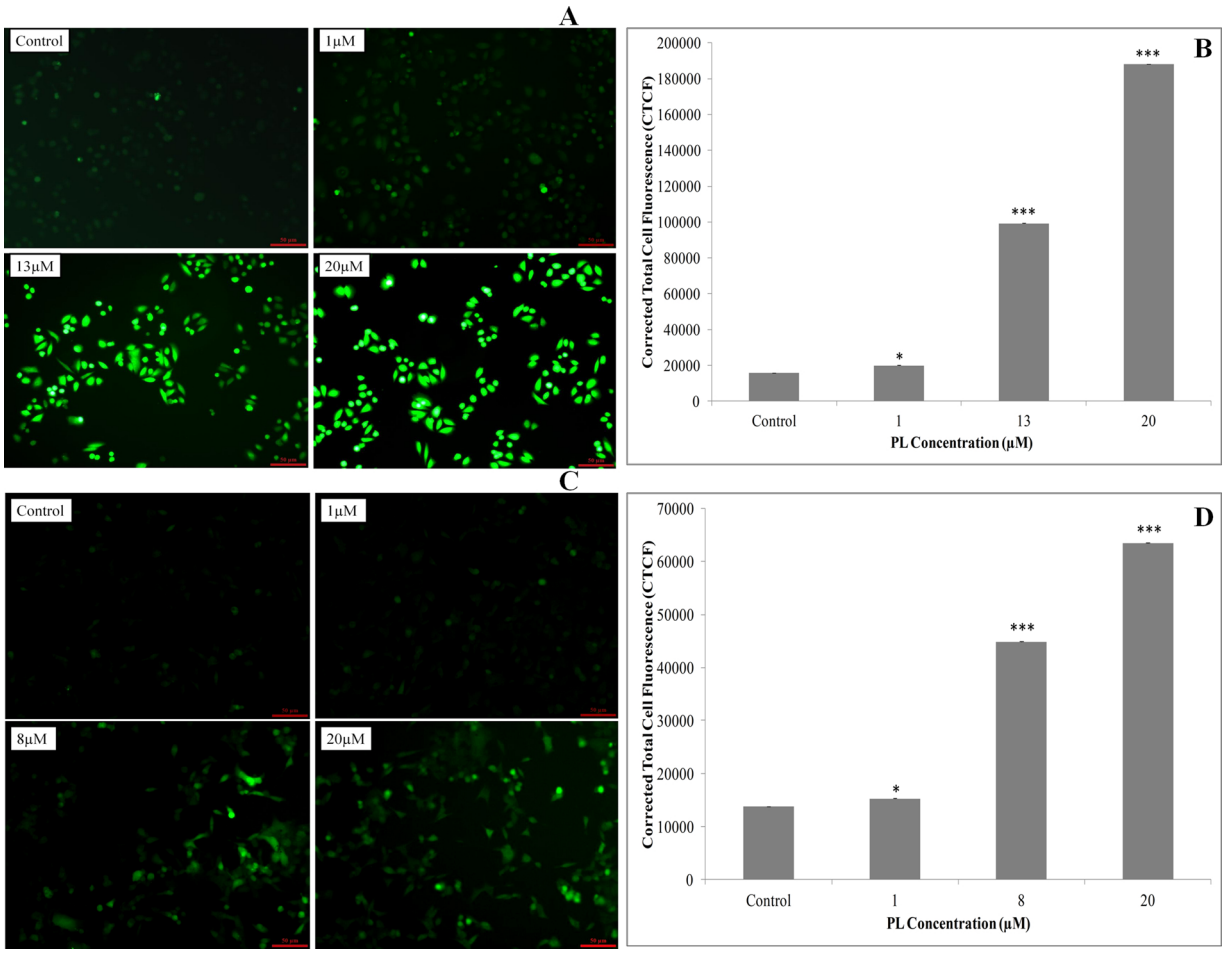

Fig. 4. Intracellular ROS was measured by DCFDA staining after PL treatment. Representative fluorescence images of INT-407 (A) and HCT-116 (C) cells. (B) & (D) show the quantified data of (A) & (C) respectively. The intensity of the green fluorescence indicates ROS concentration in the cells. Data represented as the mean ± SE of three independent experiments (statistically significant differences, * $P < 0.05$, ** $P < 0.01$, *** $P < 0.001$).

3.2. Piperlongumine promotes cell death in human intestinal cancer cells

The number of viable and dead cells was determined by using the acridine orange and propidium iodide double staining method. The stained cells were visualized under a fluorescence microscope. The viable cells with intact membrane showed green fluorescence while the membrane compromised and dead cells produced yellow-orange and red fluorescence, respectively. The number of viable and membrane compromised/dead cells were counted from three random microscopic fields per sample and the results were expressed as a percentage of live/dead cells (Fig. 2A and C). This study reveals that with increasing doses of PL treatment the number of dead cells increased significantly in both INT-407 and HCT-116 cell lines as compared to respective controls (Fig. 2B and D). These results suggested that PL triggers cell death in intestinal cancerous cells.

3.3. Piperlongumine induces nuclear damage and chromatin condensation

To determine the changes in nuclear morphology upon PL treatment, we stained the cells with a DNA binding dye Hoechst 33258 and observed under microscope. The nuclei of untreated cells were normal in both size and shape. However, the PL-treated cells showed condensed or fragmented nuclei (Fig. 3A and C). The number of fragmented and deformed cell nuclei increased significantly at 8 μM (IC_{50} for HCT-116), 13 μM (IC_{50} for INT-407) and 20 μM doses of PL (Fig. 3B and D). This indicated that piperlongumine can induce morphological changes, chromatin condensation and nuclear fragmentation in both INT-407 and HCT-116 cells (Fig. 3). Furthermore, these results suggest that the non-repairable nuclear damages can trigger cell death by apoptosis implicating PL mechanisms of action by promoting apoptosis in human intestinal cancer cells as demonstrated in other cancer cells [33,34].

3.4. Piperlongumine treatment increases intracellular ROS level

The intracellular ROS levels in control and PL-treated cells were examined using the DCFDA fluorescent dye. The fluorescence intensity had increased significantly when INT-407 and HCT-116 intestinal cancer cells were treated with PL as compared to the untreated controls, where DCFDA fluorescence was nearly negligible. At 20 μM PL, the highest dose used in this study, the INT-407 cells produced high levels of ROS as compared to the HCT-116 cells (Fig. 4), which may be the reason for the higher sensitivity of HCT-116 to PL as compared to INT-407. These results suggest that PL is able to increase the intracellular ROS levels sufficient enough to cause lethal oxidative stress in cells and which make cancer cells vulnerable to apoptosis.

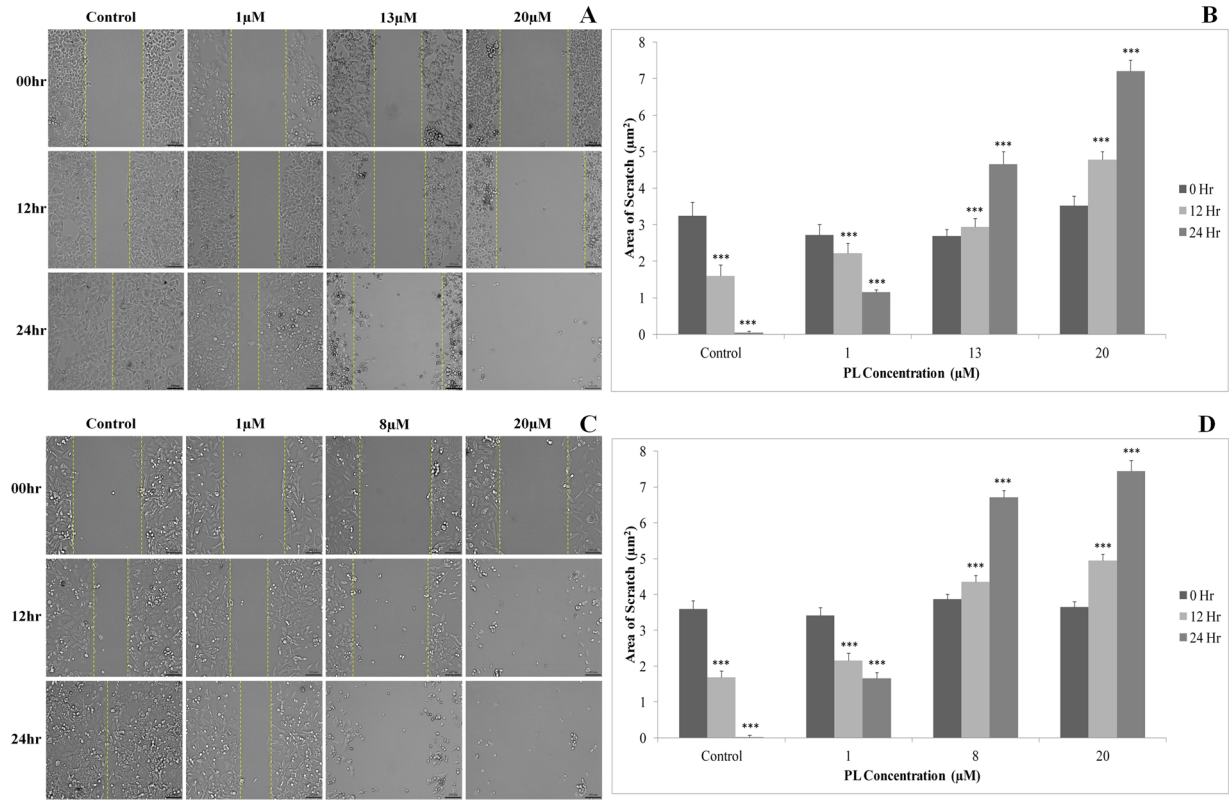

Fig. 5. Migration ability of cancer cells was determined by wound healing assay after PL treatment. Images were captured at 0, 12 and 24 h time points. Representative brightfield micrographs of INT-407 (A) and HCT-116 (C) cells indicating migration. The histograms (B) & (D) represent quantified wound area (μm^2) of (A) & (C) respectively. Data represented as the mean ± SE of three independent experiments (statistically significant differences, *$P < 0.05$, ** $P < 0.01$, *** $P < 0.001$).

3.5. Piperlongumine suppresses migration of cancer cell

Wound healing assay was performed to check the effect of PL on the migration of INT-407 and HCT-116 intestinal cancer cells. PL treatment reduced the migration ability of both the cell lines (INT-407 and HCT-116) even at the lowest treatment dose *i.e.* 1 μM. With the increasing PL doses (8 μM for HCT-116, 13 μM for INT-407 and 20 μM) and treatment timings, migration ability was reduced and the wound size also drastically increased because of enhanced cell death (Fig. 5A and C). The data shows that, both the PL treated intestinal cancer cell lines exhibited a statistically significant reduction in migration ability (Fig. 5B and D). While, the untreated cells displayed normal migration ability and the wound was completely healed within 24 h.

3.6. Effect on gene expression upon Piperlongumine treatment

Real-time PCR was performed to check mRNA levels of some tumor suppressor, pro-apoptotic and anti-apoptotic genes in PL-treated INT-407 and HCT-116 intestinal cancer cells. The expression of pro-apoptotic gene BAX was increased by 2.6 and 2.1 folds in INT-407 and HCT-116 respectively. Interestingly, the expression of both the anti-apoptotic genes *BCL2* and *SURVININ* was decreased by 3.5 folds in PL treated INT-407 cells, whereas in HCT-116 cells, 2.3 and 5.7 folds down-expression was observed for *BCL2* and *SURVININ* genes respectively. Moreover, the expression of the tumor suppressor gene *P53* was upregulated by 2.2 and 1.4 folds in INT-407 and HCT-116 cells respectively. The Expression of cell cycle regulator gene *P21* was increased 5.9 folds in INT-407 and 1.4 folds in HCT-116 after PL treatment. Additionally, the *SMAD4* expression was increased by 2.8 and 4.7 folds in INT-407 and HCT-116 cells after PL treatment. The mRNA expression of genes after PL treatment was found to be statistically significant for both the cell lines. Also, the expression of migration marker genes in PL-treated INT-407 cells was decreased, *FN1* (2.6 fold), *CDH2* (3.1 fold), *CTNNB1* (4.4 fold) and *TWIST* (3.2 fold). Similarly, a significant reduction in the expression of *FN1* (11.5 fold), *CDH2* (6 fold), *CTNNB1* (11.5 fold) and *TWIST* (13.5 fold) genes was found in HCT-116 cells upon PL exposure. Above results further suggest that PL kills intestinal cancer cells by inducing apoptosis (Fig. 6).

3.7. Piperlongumine synergized with paclitaxel in intestinal cancer cells

The combination therapy of drugs can reduce the adverse effects of chemotherapy as it reduces the drug dose. Therefore, novel combination of chemotherapeutic agents is required to conquer drug resistance and to achieve the significant therapeutic effects. Currently, Paclitaxel (PTX) is one of the mainstream chemotherapeutic drug for cancer treatment. Current study proved that the combination of two drugs (PL + PTX) at lower dose exerted a synergistic anti-cancer response

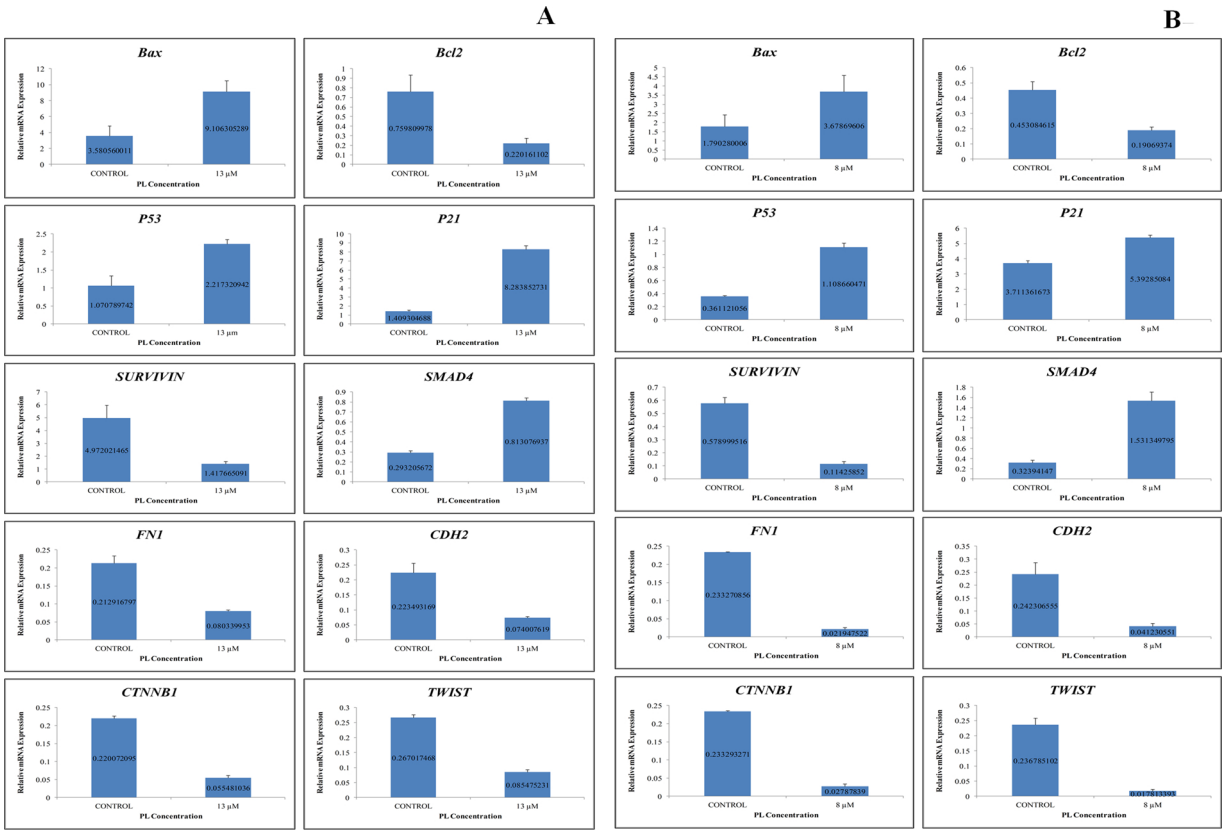

Fig. 6. Relative mRNA expression of *BAX, BCl2, P53, P21, SURVIVIN*, *SMAD4, FN1, CDH2, CTNNB1* and *TWIST* genes with respect to *18s* rRNA after 24 h piperlongumine treatment. Histograms represent normalized fold change in gene expression in INT-407 (A) and HCT-116 (B). Data represented as the mean ± SE of three independent experiments.

compared to PL or PTX treatment alone. INT-407 and HCT-116 cells were exposed with 1 to 5 µM PL combined with 0.1 to 1 µM PTX followed by MTT assay to determine cytotoxicity.

The obtained data was analyzed for synergy via bioinformatics tools (SynergyFinder and CompuSyn). The viability of both the intestinal cancer cell lines was declined significantly in all PL (1, 2.5 and 5µM) and PTX (0.1, 0.5 and 1 µM) combinations. Heat maps showed the percentage of inhibition in the different combinations. Further, Synergy maps, dose effect curves and isobolograms were plotted, which suggest the synergy score, effect of doses and combination index respectively (Figs. 7 and 8, Tables 1 and 2). The CI values for all the doses found to be less than 1 that suggested synergistic effect of PL and PTX combinations. These findings confirmed that PL was able to sensitize INT-407 and HCT-116 cancer cells to Paclitaxel in the drug dose 0.1 to 1 µM.

4. Discussion

The selective killing of cancer cells by PL has been explored and found to be ROS dependent in many cancer models [13,35]. But the effect of PL on intestinal carcinoma is still unexplored. We have brought forth some evidence to suggest that PL has greater potency to human intestinal cancer cells and PL effect is disturbing ROS homeostasis in the cancer cells. As we know that ROS are essential for several cellular processes [5,6], the imbalance of redox homeostasis can cause non-repairable damages to cell, that are associated with carcinogenesis, metastasis, and therapeutic resistance [36]. The PL exposure is known to enhance ROS production in the cancerous cells and suppresses antioxidant enzymes [18], leading to the change in ROS homeostasis in other cancers. Our results on MTT and AO/PI assays also showed the reduced cell viability for both the cell lines (INT-407 & HCT-116) upon PL treatment, which was concurred with the increase in the levels of DCFDA fluorescence. This suggested that PL works in intestinal cancer as an anticancer agent by employed nearly similar metabolic response of ROS elevation as known in other cancers.

Several studies have shown that the upregulation of SMAD4 restrict tumorigenesis [37,38] whereas, its inactivation promotes malignancy and drug resistance [39]. So, in the present study the expression of SMAD4 along with other genes such as *P21*, *BAX, BCL2*, and *SURVIVIN* was checked in the PL treated cells at 24 h. p21 is one of the important cell cycle regulators which induce senescence and considered as a checkpoint for limiting the growth of cancer cells [40], whereas *BAX, BCL2* and *SURVIVIN* exhibit crucial role in apoptotic regulation [41,42]. Reports indicate that the upregulation of SMAD4 enhances p21 expression which inhibits Bcl2 and Survivin and this inhibition will result in apoptosis [38,43,44]. As per the reports, we also observed a significant increase in the mRNA expression level of *SMAD4, BAX,* and *P21*. While a decrease in the expression of *BCL2* and *SURVIVIN* was observed upon PL treatment at 24 h. *BAX* and *BCL2*, members of the bcl-2 gene family are reported to act antagonistically [45]. The expression data from our study also shows a similar trend. The

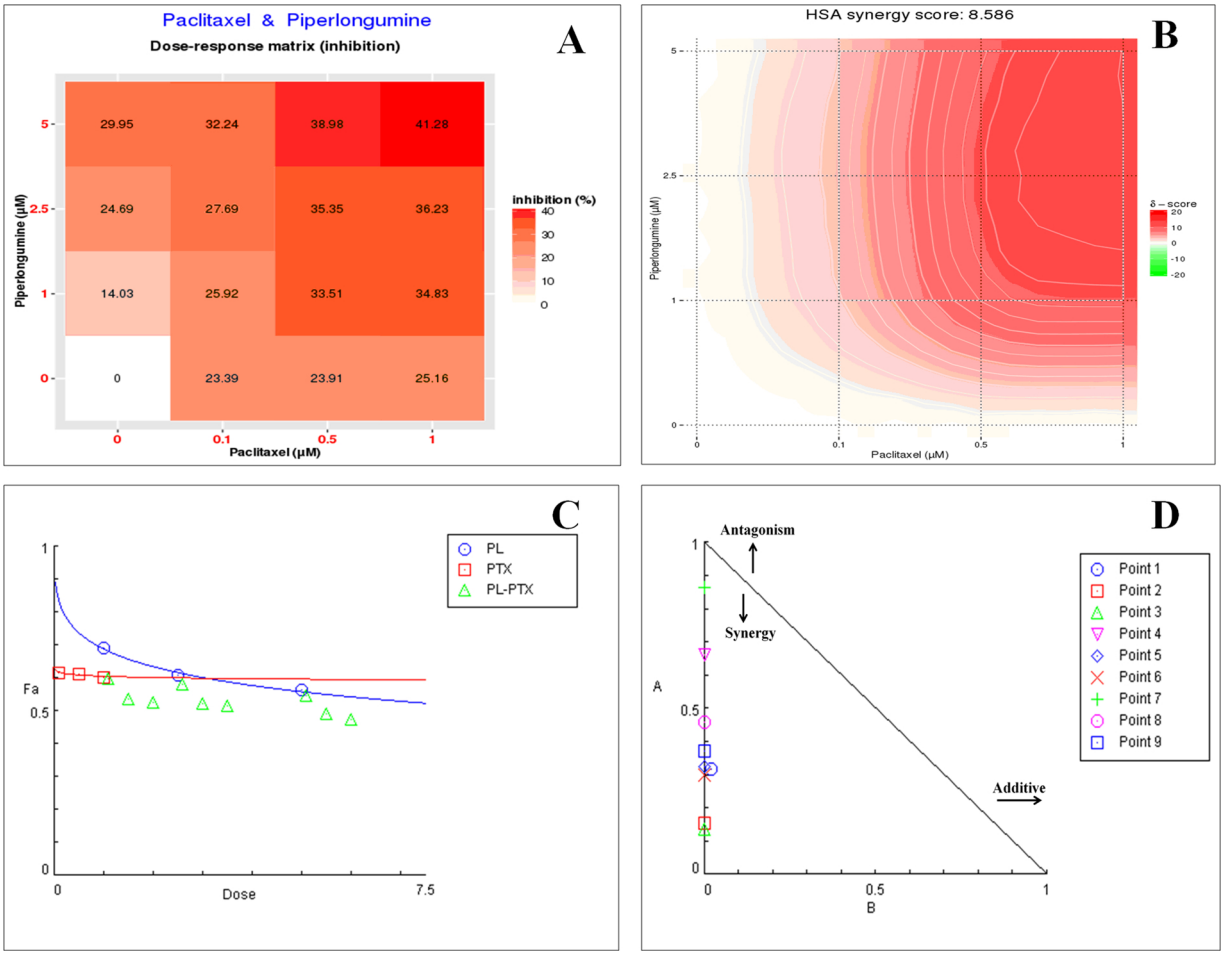

Fig. 7. PL synergized with PTX in INT-407 cancer cells. The data were analyzed by SynergyFinder and CompuSyn tools. (A) Dose response matrix showed inhibition pattern. (B) HSA Synergy plot and score. (C) Dose-effect curve. (D) Normalized isobologram.

upregulation of *BAX* and down-regulation of *BCL2* will lead to apoptosis on PL treatment. These findings suggest that PL can also plausibly act via the SMAD4 pathway. Also, the down-regulation of genes *FN1*, *CDH2*, *CTNNB1*, and *TWIST* are well-known markers for the migration and invasive properties in the cancer cells. Their down regulation after PL treatment further demonstrates the potential roles of PL in regulation of intestinal cancer cells migration as reported for other cancer models [46–52].

The current study also indicates that PL synergizes with paclitaxel. As paclitaxel is a first-line chemotherapeutic drug administered for cancer treatment, the combination of paclitaxel and PL may promise potential efficacy in the clinical trials. This report is the first to show that PL potentiates the cytotoxicity of paclitaxel in intestinal cancer cells. PL induced a significant increase in paclitaxel-mediated cell death even at lower concentrations. The required dose of paclitaxel can be reduced by PL in the clinical settings and thereby minimizing the adverse side effects of paclitaxel in chemotherapy. These facts suggest administration of paclitaxel along with PL can be very promising from the clinical point of view.

In summary, the results presented here suggest that PL acts through one or all of the three mechanisms in intestinal cancer cells such as (1) By increasing ROS levels, which would lead to DNA fragmentation and hence activating *P53* which then triggers apoptosis [53], (2) by inhibiting the antioxidant enzymes, leading to elevation of ROS levels and eventually cell death, and (3) by activating the SMAD4 pathway, which would have increased chemotherapeutic response of intestinal cancer cells by activating p21 and its downstream pathways leading to apoptosis. In conclusion, the study states that PL inhibits proliferation of intestinal cancer cells (INT-407 and HCT-116) by initiating ROS production which leads to DNA damage and interruption in cell signaling. The results depict anti-cancer potential of PL against human intestinal carcinoma and could be used as a potential therapeutic drug. Also, piperlongumine in combination with paclitaxel can be a better option for future intestinal cancer treatment.

Declaration of Competing Interest

The authors disclose no potential conflict of interest.

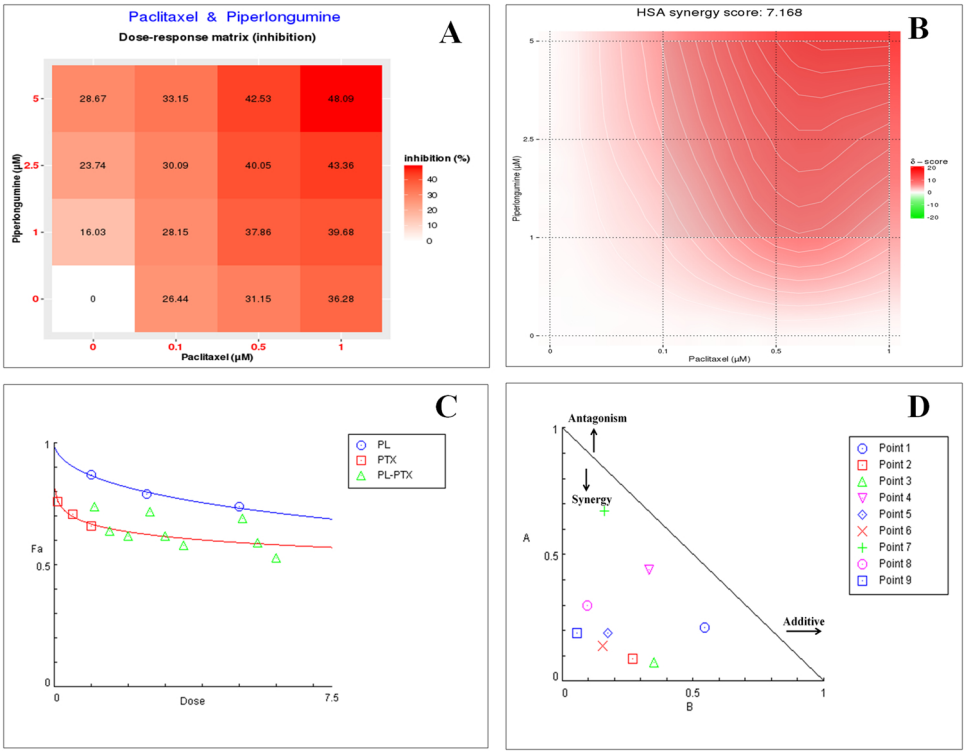

Fig. 8. PL synergized with PTX in HCT-116 cancer cells. The data were analyzed by SynergyFinder and CompuSyn tools. (A) Dose response matrix showed inhibition pattern. (B) HSA Synergy plot and score. (C) Dose-effect curve. (D) Normalized isobologram.

Table 1
Combination index of PL-PTX in INT-407.

Dose PL	Dose PTX	Effect	CI
1.0	0.1	0.74	0.75931
1.0	0.5	0.64	0.35828
1.0	1.0	0.62	0.42913
2.5	0.1	0.72	0.77217
2.5	0.5	0.62	0.36549
2.5	1.0	0.58	0.29393
5.0	0.1	0.69	0.83626
5.0	0.5	0.59	0.39388
5.0	1.0	0.53	0.24694

Table 2
Combination index of PL-PTX in HCT-116.

Dose PL	Dose PTX	Effect	CI
1.0	0.1	0.74	0.75931
1.0	0.5	0.64	0.35828
1.0	1.0	0.62	0.42913
2.5	0.1	0.72	0.77217
2.5	0.5	0.62	0.36549
2.5	1.0	0.58	0.29393
5.0	0.1	0.69	0.83626
5.0	0.5	0.59	0.39388
5.0	1.0	0.53	0.24694

Acknowledgments

Authors would like to thank the Birla Institute of Technology and Science, Pilani, K.K. Birla Goa Campus to provide the space to perform this study and Central Sophisticated Instrumentation Facility (CSIF) for confocal microscopy. Funding for the work was provided by the Department of Science and Technology (project number: SB/SO/BB/103/2013), Government of India.

Appendix A. Supplementary data

Supplementary material related to this article can be found, in the online version, at doi:https://doi.org/10.1016/j.biopha.2020.110243.

References

[1] R.L. Siegel, K.D. Miller, A. Jemal, Cancer statistics, 2018, CA Cancer J. Clin. 68 (2018) 7–30, https://doi.org/10.3322/caac.21442.
[2] W.-H. Chow, M.S. Linet, J.K. McLaughlin, A.W. Hsing, H.T. Co Chien, W.J. Blot, Risk factors for small intestine cancer, Cancer Causes Control 4 (1993) 163–169, https://doi.org/10.1007/BF00053158.
[3] R.L. Siegel, K.D. Miller, S.A. Fedewa, D.J. Ahnen, R.G.S. Meester, A. Barzi, A. Jemal, Colorectal cancer statistics, CA Cancer J. Clin. 67 (2017) (2017) 177–193, https://doi.org/10.3322/caac.21395.
[4] M. Der Shi, H.H. Lin, Y.C. Lee, J.K. Chao, R.A. Lin, J.H. Chen, Inhibition of cell-cycle progression in human colorectal carcinoma Lovo cells by andrographolide, Chem. Biol. Interact. 174 (2008) 201–210, https://doi.org/10.1016/j.cbi.2008.06.006.
[5] L. Sena, N. Chandel, Physiological roles of mitochondrial reactive oxygen species, Mol. Cell 48 (2012) 158–167, https://doi.org/10.1016/j.molcel.2012.09.025. Physiological.
[6] H. Wiseman, B. Halliwell, Damage to DNA by reactive oxygen and nitrogen species: role in inflammatory disease and progression to cancer, Biochem. J. 313 (Pt 1) (1996) 17–29, https://doi.org/10.1038/srep09969.
[7] D. Trachootham, J. Alexandre, P. Huang, Targeting cancer cells by ROS mediated mechanisms: a radical therapeutic approach? Nat. Rev. Drug Discov. 8 (2009) 579–591 (Accessed April 19, 2018), https://www.nature.com/articles/nrd2803.
[8] G.M. Denicola, F.A. Karreth, T.J. Humpton, A. Gopinathan, C. Wei, K. Frese, D. Mangal, K.H. Yu, C.J. Yeo, E.S. Calhoun, F. Scrimieri, J.M. Winter, R.H. Hruban, C. Iacobuzio-Donahue, S.E. Kern, I.A. Blair, D.A. Tuveson, Oncogene-induced Nrf2 transcription promotes ROS detoxification and tumorigenesis, Nature 475 (2011) 106–110, https://doi.org/10.1038/nature10189.
[9] M. Jeanne, V. Lallemand-Breitenbach, O. Ferhi, M. Koken, M. Le Bras, S. Duffort, L. Peres, C. Berthier, H. Soilihi, B. Raught, H. de Thé, PML/RARA oxidation and arsenic binding initiate the antileukemia response of As2O3, Cancer Cell 18 (2010) 88–98, https://doi.org/10.1016/j.ccr.2010.06.003.
[10] J. Alexandre, Y. Hu, W. Lu, H. Pelicano, P. Huang, Novel action of paclitaxel against cancer cells: bystander effect mediated by reactive oxygen species, Cancer Res. 67 (2007) 3512–3517, https://doi.org/10.1158/0008-5472.CAN-06-3914.
[11] J. Saczko, A. Choromańska, N. Rembiałkowska, M. Dubińska-Magiera, I. Bednarz-Misa, J. Bar, A. Marcinkowska, J. Kulbacka, Oxidative modification induced by photodynamic therapy with Photofrin®II and 2-methoxyestradiol in human ovarian clear carcinoma (OvBH-1) and human breast adenocarcinoma (MCF-7) cells, Biomed. Pharmacother. 71 (2015) 30–36, https://doi.org/10.1016/j.biopha.2015.

02.008.
[12] D.P. Bezerra, C. Pessoa, M.O. De Moraes, N. Saker-Neto, E.R. Silveira, L.V. Costa-Lotufo, Overview of the therapeutic potential of piplartine (piperlongumine), Eur. J. Pharm. Sci. 48 (2013) 453–463, https://doi.org/10.1016/j.ejps.2012.12.003.
[13] J.M. Liu, F. Pan, L. Li, Q.R. Liu, Y. Chen, X.X. Xiong, K. Cheng, S. Bin Yu, Z. Shi, A.C.H. Yu, X.Q. Chen, Piperlongumine selectively kills glioblastoma multiforme cells via reactive oxygen species accumulation dependent JNK and p38 activation, Biochem. Biophys. Res. Commun. 437 (2013) 87–93, https://doi.org/10.1016/j.bbrc.2013.06.042.
[14] U. Bharadwaj, T.K. Eckols, M. Kolosov, M.M. Kasembeli, A. Adam, D. Torres, X. Zhang, L.E. Dobrolecki, W. Wei, M.T. Lewis, B. Dave, J.C. Chang, M.D. Landis, C.J. Creighton, M.A. Mancini, D.J. Tweardy, Drug-repositioning screening identified piperlongumine as a direct STAT3 inhibitor with potent activity against breast cancer, Oncogene. 34 (2015) 1341–1353, https://doi.org/10.1038/onc.2014.72.
[15] H. Randhawa, K. Kibble, H. Zeng, M.P. Moyer, K.M. Reindl, Activation of ERK signaling and induction of colon cancer cell death by piperlongumine, Toxicol. In Vitro 27 (2013) 1626–1633, https://doi.org/10.1016/j.tiv.2013.04.006.
[16] S. Shrivastava, P. Kulkarni, D. Thummuri, M.K. Jeengar, V.G.M. Naidu, M. Alvala, G.B. Redddy, S. Ramakrishna, Piperlongumine, an alkaloid causes inhibition of PI3 K/Akt/mTOR signaling axis to induce caspase-dependent apoptosis in human triple-negative breast cancer cells, Apoptosis 19 (2014) 1148–1164, https://doi.org/10.1007/s10495-014-0991-2.
[17] P. Makhov, K. Golovine, E. Teper, A. Kutikov, R. Mehrazin, A. Corcoran, A. Tulin, R.G. Uzzo, V.M. Kolenko, Piperlongumine promotes autophagy via inhibition of Akt/mTOR signalling and mediates cancer cell death, Br. J. Cancer 110 (2014) 899–907, https://doi.org/10.1038/bjc.2013.810.
[18] P. Zou, Y. Xia, J. Ji, W. Chen, J. Zhang, X. Chen, V. Rajamanickam, G. Chen, Z. Wang, L. Chen, Y. Wang, S. Yang, G. Liang, Piperlongumine as a direct TrxR1 inhibitor with suppressive activity against gastric cancer, Cancer Lett. 375 (2016) 114–126, https://doi.org/10.1016/j.canlet.2016.02.058.
[19] Y. Wang, X. Wu, Y. Zhou, H. Jiang, S. Pan, B. Sun, Piperlongumine suppresses growth and sensitizes pancreatic tumors to gemcitabine in a xenograft mouse model by modulating the NF-kappa B pathway, Cancer Prev. Res. Phila. 9 (2016) 234–244, https://doi.org/10.1158/1940-6207.CAPR-15-0306.
[20] J. Massagué, TGFβ in Cancer, Cell. 134 (2008) 215–230, https://doi.org/10.1016/j.cell.2008.07.001.
[21] B. Zhang, S.K. Halder, S. Zhang, P.K. Datta, Targeting transforming growth factor-beta signaling in liver metastasis of colon cancer, Cancer Lett. 277 (2009) 114–120, https://doi.org/10.1016/j.canlet.2008.11.035.
[22] L. Losi, H. Bouzourene, J. Benhattar, Loss of Smad4 expression predicts liver metastasis in human colorectal cancer, Oncol. Rep. 17 (2007) 1095–1099, https://doi.org/10.3892/or.17.5.1095.
[23] H. Alazzouzi, P. Alhopuro, R. Salovaara, H. Sammalkorpi, H. Järvinen, J.P. Mecklin, A. Hemminki, S. Schwartz, L.A. Aaltonen, D. Arango, SMAD4 as a prognostic marker in colorectal cancer, Clin. Cancer Res. 11 (2005) 2606–2611, https://doi.org/10.1158/1078-0432.CCR-04-1458.
[24] B. Zhang, B. Zhang, X. Chen, S. Bae, K. Singh, M.K. Washington, P.K. Datta, Loss of Smad4 in colorectal cancer induces resistance to 5-fluorouracil through activating Akt pathway, Br. J. Cancer 110 (2014) 946–957, https://doi.org/10.1038/bjc.2013.789.
[25] T.C. Chou, Drug combination studies and their synergy quantification using the chou-talalay method, Cancer Res. 70 (2010) 440–446, https://doi.org/10.1158/0008-5472.CAN-09-1947.
[26] A. Ianevski, L. He, T. Aittokallio, J. Tang, SynergyFinder: A web application for analyzing drug combination dose-response matrix data, Bioinformatics. 33 (2017) 2413–2415, https://doi.org/10.1093/bioinformatics/btx162.
[27] R. Supino, MTT assays, Vitr. Toxic. Test. Protoc. Humana Press, Totowa, NJ, 2009, pp. 137–149, https://doi.org/10.1385/0-89603-282-5:137.
[28] H.L. Bank, Rapid assessment of islet viability with acridine orange and propidium iodide, Vitr. Cell. Dev. Biol. 24 (1988) 266–273, https://doi.org/10.1007/BF02628826.
[29] F. Li, J.H. Wu, Q.H. Wang, Y.L. Shu, C.W. Wan, C.O. Chan, D. Kam-Wah Mok, S.W. Chan, Gui-ling-gao, a traditional Chinese functional food, prevents oxidative stress-induced apoptosis in H9c2 cardiomyocytes, Food Funct. 4 (2013) 745–753, https://doi.org/10.1039/c3fo30182f.
[30] L. Sun, C. Luo, J. Liu, Hydroxytyrosol induces apoptosis in human colon cancer cells through ROS generation, Food Funct. 5 (2014) 1909–1914, https://doi.org/10.1039/c4fo00187g.
[31] G.P. Rédei, Wound-Healing Assay, in: Encycl. Genet. Genomics, Proteomics Informatics, Humana Press, New Jersey, 2008, p. 2108, https://doi.org/10.1007/978-1-4020-6754-9_18201 2108.
[32] K.J. Livak, T.D. Schmittgen, Analysis of relative gene expression data using real-time quantitative PCR and the 2-ΔΔCT method, Methods 25 (2001) 402–408, https://doi.org/10.1006/meth.2001.1262.
[33] H. Dhillon, S. Chikara, K.M. Reindl, Piperlongumine induces pancreatic cancer cell death by enhancing reactive oxygen species and DNA damage, Toxicol. Rep. (2014), https://doi.org/10.1016/j.toxrep.2014.05.011.
[34] S. Okamoto, T. Narita, H. Sasanuma, S. Takeda, S.I. Masunaga, T. Bessho, K. Tano, Impact of DNA repair pathways on the cytotoxicity of piperlongumine in chicken DT40 cell-lines, Genes Cancer (2014), https://doi.org/10.18632/genesandcancer.26.
[35] Y. Chen, J.M. Liu, X.X. Xiong, X.Y. Qiu, F. Pan, D. Liu, S.J. Lan, S. Jin, S. Bin Yu, X.Q. Chen, Piperlongumine selectively kills hepatocellular carcinoma cells and preferentially inhibits their invasion via ROS-ER-MAPKs-CHOP, Oncotarget 6 (2015) 6406–6421, https://doi.org/10.18632/oncotarget.3444.
[36] M. Valko, D. Leibfritz, J. Moncol, M.T.D. Cronin, M. Mazur, J. Telser, Free radicals and antioxidants in normal physiological functions and human disease, Int. J. Biochem. Cell Biol. 39 (2007) 44–84, https://doi.org/10.1016/j.biocel.2006.07.001.
[37] B. Zhang, B. Zhang, X. Chen, S. Bae, K. Singh, M.K. Washington, P.K. Datta, Loss of Smad4 in colorectal cancer induces resistance to 5-fluorouracil through activating Akt pathway, Br. J. Cancer 110 (2014) 946–957, https://doi.org/10.1038/bjc.2013.789.
[38] K.K. Hunt, J.B. Fleming, A. Abramian, L. Zhang, D.B. Evans, P.J. Chiao2, Overexpression of the Tumor Suppressor Gene Smad4/DPC4 Induces p2T"afl Expression and Growth Inhibition in Human Carcinoma Cells 1, (1998) (Accessed February 2, 2019), http://cancerres.aacrjournals.org/content/canres/58/24/5656.full.pdf.
[39] P. Papageorgis, K. Cheng, S. Ozturk, Y. Gong, A.W. Lambert, H.M. Abdolmaleky, J.R. Zhou, S. Thiagalingam, Smad4 inactivation promotes malignancy and drug resistance of colon cancer, Cancer Res. 71 (2011) 998–1008, https://doi.org/10.1158/0008-5472.CAN-09-3269.
[40] J. Boulaire, A. Fotedar, R. Fotedar, The functions of the cdk-cyclin kinase inhibitor p21WAF1, Pathol Biol (Paris) 4 (April (2000)) (2000) 190–202 (Accessed May 13, 2018), http://www.ncbi.nlm.nih.gov/pubmed/10858953.
[41] M.S. Ola, M. Nawaz, H. Ahsan, Role of Bcl-2 family proteins and caspases in the regulation of apoptosis, Mol. Cell. Biochem. 351 (2011) 41–58, https://doi.org/10.1007/s11010-010-0709-x.
[42] A.C. Mita, M.M. Mita, S.T. Nawrocki, F.J. Giles, Survivin: Key regulator of mitosis and apoptosis and novel target for cancer therapeutics, Clin. Cancer Res. 14 (2008) 5000–5005, https://doi.org/10.1158/1078-0432.CCR-08-0746.
[43] Y. Tan, L. Wang, Y. Du, X. Liu, Z. Chen, X. Weng, J. Guo, H. Chen, M. Wang, X. Wang, Inhibition of BRD4 suppresses tumor growth in prostate cancer via the enhancement of FOXO1 expression, Int. J. Oncol. 53 (2018) 2503–2517, https://doi.org/10.3892/ijo.2018.4577.
[44] T. Muramatsu, I. Imoto, T. Matsui, K.I. Kozaki, S. Haruki, M. Sudol, Y. Shimada, H. Tsuda, T. Kawano, J. Inazawa, YAP is a candidate oncogene for esophageal squamous cell carcinoma, Carcinogenesis 32 (2011) 389–398, https://doi.org/10.1093/carcin/bgq254.
[45] B. Kulsoom, T.S. Shamsi, N.A. Afsar, Z. Memon, N. Ahmed, S.N. Hasnain, Bax, Bcl-2, and Bax/Bcl-2 as prognostic markers in acute myeloid leukemia: Are we ready for bcl-2-directed therapy? Cancer Manag. Res. 10 (2018) 403–416, https://doi.org/10.2147/CMAR.S154608.
[46] M. Sponziello, F. Rosignolo, M. Celano, V. Maggisano, V. Pecce, R.F. De Rose, G.E. Lombardo, C. Durante, S. Filetti, G. Damante, D. Russo, S. Bulotta, Fibronectin-1 expression is increased in aggressive thyroid cancer and favors the migration and invasion of cancer cells, Mol. Cell. Endocrinol. 431 (2016) 123–132, https://doi.org/10.1016/j.mce.2016.05.007.
[47] N.G. Yousif, Fibronectin promotes migration and invasion of ovarian cancer cells through up-regulation of FAK-PI3K/Akt pathway, Cell Biol. Int. 38 (2014) 85–91, https://doi.org/10.1002/cbin.10184.
[48] M. Jeon, J. Lee, S.J. Nam, I. Shin, J.E. Lee, S. Kim, Induction of fibronectin by HER2 overexpression triggers adhesion and invasion of breast cancer cells, Exp. Cell Res. 333 (2015) 116–126, https://doi.org/10.1016/j.yexcr.2015.02.019.
[49] J. Xu, J.R. Prosperi, N. Choudhury, O.I. Olopade, K.H. Goss, β-catenin is required for the tumorigenic behavior of triple-negative breast cancer cells, PLoS One 10 (2015) e0117097, , https://doi.org/10.1371/journal.pone.0117097.
[50] N.R. Alexander, N.L. Tran, H. Rekapally, C.E. Summers, C. Glackin, R.L. Heimark, N-cadherin gene expression in prostate carcinoma is modulated by integrin-dependent nuclear translocation of Twist1, Cancer Res. 66 (2006) 3365–3369, https://doi.org/10.1158/0008-5472.CAN-05-3401.
[51] Z. Yang, X. Zhang, H. Gang, X. Li, Z. Li, T. Wang, J. Han, T. Luo, F. Wen, X. Wu, Up-regulation of gastric cancer cell invasion by Twist is accompanied by N-cadherin and fibronectin expression, Biochem. Biophys. Res. Commun. 358 (2007) 925–930, https://doi.org/10.1016/j.bbrc.2007.05.023.
[52] W.K. Kwok, M.T. Ling, T.W. Lee, T.C.M. Lau, C. Zhou, X. Zhang, C.W. Chua, K.W. Chan, F.L. Chan, C. Glackin, Y.C. Wong, X. Wang, Up-regulation of TWIST in prostate cancer and its implication as a therapeutic target, Cancer Res. 65 (2005) 5153–5162, https://doi.org/10.1158/0008-5472.CAN-04-3785.
[53] W.P. Roos, B. Kaina, DNA damage-induced cell death by apoptosis, Trends Mol. Med. 12 (2006) 440–450, https://doi.org/10.1016/j.molmed.2006.07.007.